

# A myocardium tropic adeno-associated virus (AAV) evolved by DNA shuffling and in vivo selection

Lin Yang<sup>a</sup>, Jiangang Jiang<sup>a</sup>, Lauren M. Drouin<sup>b</sup>, Mavis Agbandje-Mckenna<sup>b</sup>, Chunlian Chen<sup>a</sup>, Chunping Qiao<sup>a</sup>, Dongqiye Pu<sup>a</sup>, Xiaoyun Hu<sup>c</sup>, Da-Zhi Wang<sup>c</sup>, Juan Li<sup>a</sup>, and Xiao Xiao<sup>a,1</sup>

<sup>a</sup>Division of Molecular Pharmaceutics, University of North Carolina Eshelman School of Pharmacy, Chapel Hill, NC 27599; <sup>b</sup>Department of Biochemistry and Molecular Biology, College of Medicine, University of Florida, Gainesville, FL 32610; and <sup>c</sup>Carolina Cardiovascular Biology Center, University of North Carolina, Chapel Hill, NC 27599

Communicated by Yuet Wai Kan, University of California, San Francisco School of Medicine, San Francisco, CA, January 4, 2009 (received for review September 4, 2008)

To engineer gene vectors that target striated muscles after systemic delivery, we constructed a random library of adeno-associated virus (AAV) by shuffling the capsid genes of AAV serotypes 1 to 9, and screened for muscle-targeting capsids by direct in vivo panning after tail vein injection in mice. After 2 rounds of in vivo selection, a capsid gene named M41 was retrieved mainly based on its high frequency in the muscle and low frequency in the liver. Structural analyses revealed that the AAVM41 capsid is a recombinant of AAV1, 6, 7, and 8 with a mosaic capsid surface and a conserved capsid interior. AAVM41 was then subjected to a side-by-side comparison to AAV9, the most robust AAV for systemic heart and muscle gene delivery; to AAV6, a parental AAV with strong muscle tropism. After i.v. delivery of reporter genes, AAVM41 was found more efficient than AAV6 in the heart and muscle, and was similar to AAV9 in the heart but weaker in the muscle. In fact, the myocardium showed the highest gene expression among all tissues tested in mice and hamsters after systemic AAVM41 delivery. However, gene transfer in non-muscle tissues, mainly the liver, was dramatically reduced. AAVM41 was further tested in a genetic cardiomyopathy hamster model and achieved efficient long-term  $\delta$ -sarcoglycan gene expression and rescue of cardiac functions. Thus, direct in vivo panning of capsid libraries is a simple tool for the de-targeting and re-targeting of viral vector tissue tropisms facilitated by acquisition of desirable sequences and properties.

Muscular dystrophies are a class of debilitating and often lethal genetic diseases because of the lack of effective treatment. Cardiomyopathy is a commonly associated pathology a main cause of premature death of the patients (1). Gene therapy for muscular dystrophy and cardiomyopathy has been actively investigated as a promising and viable therapeutic approach (2). Gene vectors based on adeno-associated virus (AAV) are the most efficient vector systems currently available for gene delivery in the muscle and heart (3–8). To realize significant benefits in muscular dystrophy patients, efficient systemic therapeutic gene delivery into striated muscles throughout the body is highly desirable. The recently identified new AAV serotypes, e.g., AAV6, 7, 8, and 9, are able to serve such a purpose after i.v. injection in animal models (5, 6, 9–12). Nonetheless, those vectors also exhibit broad tissue tropism, especially in the liver, which is a major depot for AAV vectors upon intravascular administration (5, 13). The unintended gene transfer to the liver and other tissues remains a concern for muscle-oriented systemic gene delivery. As a result, de-targeting AAVs from the non-muscle tissues and re-targeting them to the muscle and heart could reduced unwanted side effects in muscle gene therapy.

The AAV genome contains 2 viral genes, *rep* (replication) and *cap* (capsid). The *cap* gene encodes 3 overlapping capsid proteins VP1, VP2, and VP3. A large number of AAV serotypes and variants have been isolated from human and non-human primates with substantial sequence diversity among their *cap* genes (12, 14). These AAV serotypes exhibit different infectivities on various tissues. Three-dimensional (3D) structure and mutagenesis studies of several AAV serotypes have shown that the common capsid region

displays an 8-stranded (bB-bI) core  $\beta$ -barrel motif with loop insertions, which are the main determinants of AAV serotype-specific properties, such as receptor recognition, transduction efficiency and antigenic reactivity (15–17). The structural information on the capsid forms the basis for genetic engineering of novel AAV vectors. DNA shuffling has recently been used to modify viral vectors (18, 19) by introducing enormous permutations of genetic variations via in vitro recombination. The shuffled AAV mutant libraries were used for selection of desirable features such as resistance to antibody neutralization (19, 20) and improved tropism to cancer cells (21). In the above studies, however, in vitro bio-panning on cultured cells was the first, and often the only, selection accompanied by intrinsic bias and limitations. No results have been reported on direct in vivo selection of AAV mutant capsids libraries after systemic administration.

In this study, we genetically engineered an AAV *cap* gene library by DNA shuffling of different AAV serotype capsid genes. The library was directly screened in mice in vivo. AAV capsids were selected by their combined capacity of crossing the tight vasculature barriers in muscle tissues and infectivity to muscle cells. One of the mutant AAV vectors named AAVM41 was found to exhibit enhanced infectivity to cardiac muscle and diminished infectivity to the liver after systemic administration. Further testing of AAVM41 in a heart failure hamster model verified its efficiency and efficacy in therapeutic gene transfer, and demonstrated the usefulness of capsid gene DNA shuffling and direct in vivo selection.

## Results

**Direct In Vivo Panning of DNA-Shuffled AAV Library for Muscle-Targeting Capsids.** We constructed a chimeric AAV library by DNA shuffling of the capsid genes of AAV1, 2, 3, 4, 6, 7, 8, and 9, to select for combined characteristics. The infectious AAV library with shuffled capsid genes was packaged by the method of Muller *et al.* (22). DNA analysis by restriction digestions on randomly picked mutant AAV clones showed unique patterns and indicated that the vast majority of them were recombinants viable in producing AAV particles.

Although it is a common practice to use in vitro cell culture systems to screen for desirable mutant AAVs, here we solely relied on a direct in vivo screening method, because no cell culture system could simultaneously mimic the in vivo conditions (e.g., the tight endothelial lining, the differentiated muscle cells and the liver). We used adult mice for in vivo bio-panning of the AAV library. After tail vein injection of a dose of  $5 \times 10^{11}$  v.g. (viral genomes), the

Author contributions: L.Y., M.A.-M., D.-Z.W., and X.X. designed research; L.Y., J.J., L.M.D., M.A.-M., C.C., C.Q., D.P., X.H., J.L., and X.X. performed research; D.-Z.W. contributed new reagents/analytic tools; L.Y., J.J., L.M.D., C.C., C.Q., D.P., J.L., and X.X. analyzed data; and L.Y. and X.X. wrote the paper.

The authors declare no conflict of interest.

<sup>1</sup>To whom correspondence should be addressed. E-mail: xxiao@email.unc.edu.

This article contains supporting information online at [www.pnas.org/cgi/content/full/0813207106/DCSupplemental](http://www.pnas.org/cgi/content/full/0813207106/DCSupplemental).

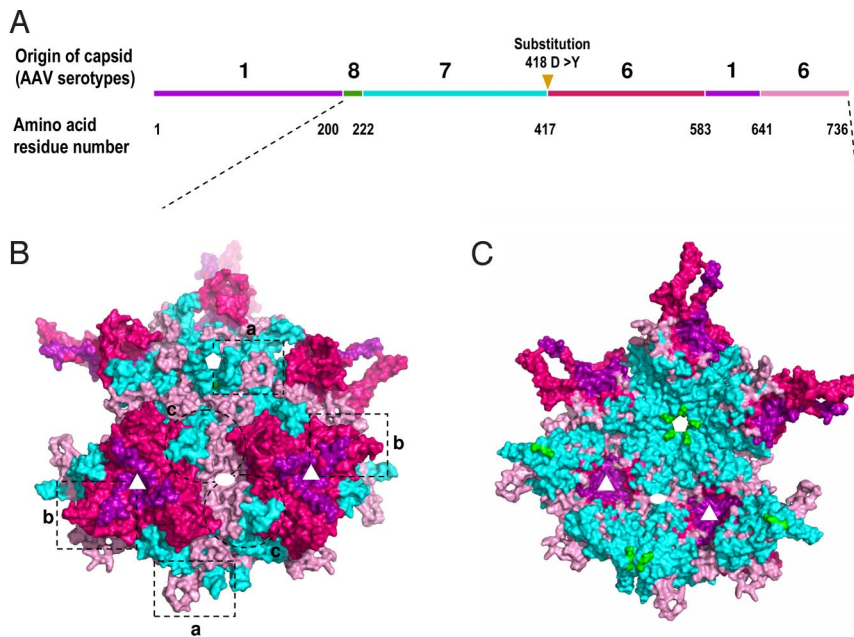


**Fig. 1.** Sequence and structure analysis of the M41 capsid. (A) The primary structure of M41 capsid by alignments of its VP1 amino acid sequence with those of the parental AAV serotypes. A D to Y substitution on residue 418 is shown by a triangle. (B and C) The structural model of the 9-mer AAVM41 VP3 subunits reconstructed from the known crystal and homologous model structures of the parental viruses with the exterior surface (B), and interior surface (C), respectively. Sequences derived from AAV1 are colored in purple, AAV6 in hot pink and light pink (2 segments), AAV7 in cyan, AAV8 in green. The axes of symmetry are shown by white pentagon (5-fold), triangle (3-fold) and oval (2-fold) on the structural models. The structural regions around them are highlighted by frames a, b, and c.

AAV *cap* genes that were enriched in the muscles were retrieved by PCR amplification. In the first round of *in vivo* screening, 43 distinct AAV clones were identified. They were mixed in equal ratio for secondary AAV library production and second-round *in vivo* screening. The clones enriched in the muscle but scarce in the liver were further characterized.

A clone named M41 appeared 12 times in 79 randomly picked clones from the muscle pool but was absent in the liver pool (Table S1). Sequence alignment of its capsid amino acid sequence showed that it is a recombinant of 4 parental AAV serotypes, AAV1, 6, 7, and 8. The *N*-terminal half of the capsid is from AAV1, 8, and 7, while the *C*-terminal half is from AAV6 and 1 (Fig. 1A). To deduce the contributions of the 4 parental serotypes, a 3D homologous structural model of M41 capsid was generated, using residues 211 to 736 of its overlapping VP1-VP3 region, by aligning its sequence with those of the parental serotypes. Both the exterior and interior surfaces of the capsid clearly showed the presence of segments from the 4 parental AAV capsids (Fig. 1B and C). On the capsid surface, the  $\beta$ DE loop of AAV7 forms the  $\beta$ -ribbons that assemble a channel at the icosahedral 5-fold axis, while AAV6 sequences form the HI loop which lies on AAV7 sequences forming the floor of the depression surrounding this axis (Fig. 1B, frame a). Three  $\beta$ GH loops with sequences from AAV1 and AAV6 interact to form the characteristic protrusions that surround the icosahedral 3-fold symmetry axis on the surface of the AAV capsid (15), with the sub-loop from AAV1 closer to the axis (Fig. 1B, frame b). The  $\beta$ BC loop from AAV7 and the region following  $\beta$ I of AAV6 form the wall between the 5- and 2-fold axes, with AAV6 forming the depression at the 2-fold axis (Fig. 1B, frame c). In contrast to the relatively complicated sequence composition on the exterior surface of the AAVM41 capsid, its interior surface was mostly composed of barrel  $\beta$ -strands from AAV7 and strand  $\beta$ I from AAV6 (Fig. 1C). The few residues from AAV8 participated in the assembly of the region of the channel at the 5-fold symmetry axis located in the interior of the capsid (Fig. 1C). This analysis highlighted the unique structural properties of the AAVM41 capsid arising from the parental serotypes.

**M41 Vector Preferentially Transduces Myocardium After Systemic Administration.** We next investigated systemic gene delivery efficiency and tissue tropism of AAVM41. The luciferase reporter gene was packaged into viral capsids of M41, AAV9, and AAV6 for a

side-by-side comparison *in vivo*. At 2 weeks post *i.v.* injection in young adult C57BJ/6L mice (6–8 wks), luciferase activities and vector DNA copy numbers in various tissues were analyzed. Consistent with previous reports (13), the AAV9 vector efficiently transduced mouse heart, skeletal muscles, and particularly the liver, which had the highest luciferase activity (Fig. 2A) and vector DNA copy numbers (Fig. 2B). Similar to AAV9, the M41 vector also transduced the heart efficiently with slightly lower luciferase activity and vector copy numbers (Fig. 2B). However, M41 showed dramatically reduced gene transfer in the liver, with the luciferase activity 81.1-fold lower and DNA copy number 11.3-fold lower than AAV9. However, AAVM41 gene transfer in the skeletal muscles, except in the tongue, was also significantly lower than AAV9 (Fig. 2A). Interestingly, although the liver had higher DNA copy numbers (Fig. 2B), the heart showed the highest luciferase activity among all tissues examined in M41 injected mice (Fig. 2A), suggesting differential intracellular trafficking and uncoating processes of AAVM41 in these 2 tissues.

Similar side-by-side comparison between AAVM41 and AAV6 at 2 weeks after *i.v.* injection revealed higher gene transfer by AAVM41 in all skeletal muscles, and dramatically higher gene transfer (>13-fold) in the heart (Fig. 2C), but >50% reduction in the liver. Interestingly, although AAV6 had significantly higher vector DNA copy numbers than AAVM41 in some muscle tissues such as the tibialis anterior and quadriceps (Ta and Qd in Fig. 2D), the gene expression levels were much lower. The inconsistency in vector genome quantity and transgene expression between these 2 viruses suggests a more complex difference in vector bioavailability in the muscle tissues, such as transcytosis through endothelial lining and preferential infection of muscle rather than non-muscle cells.

Since 1 important aim of this study was to reduce liver infectivity, we compared ratios of heart vs. liver gene expression for the above 3 AAVs. While the heart vs. liver ratio of AAVM41 was >10:1, this ratio was reversed to 1:3 in AAV9 and 1:6 in AAV6 (Fig. 2E). Consistently, the ratios of heart vs. liver vector DNA copy numbers also showed a similar trend to the luciferase activities among the 3 AAVs (Fig. 2F). These data thus demonstrated improved tropism to the heart and much reduced tropism to the liver by AAVM41.

We next used  $\beta$ -galactosidase (*LacZ*) reporter gene to directly visualize transgene expression in cardiomyocytes and myofibers. At 2 weeks post vector *i.v.* injection in adult C57BJ/6L mice, approximately one-half of the cardiomyocytes in the heart showed positive

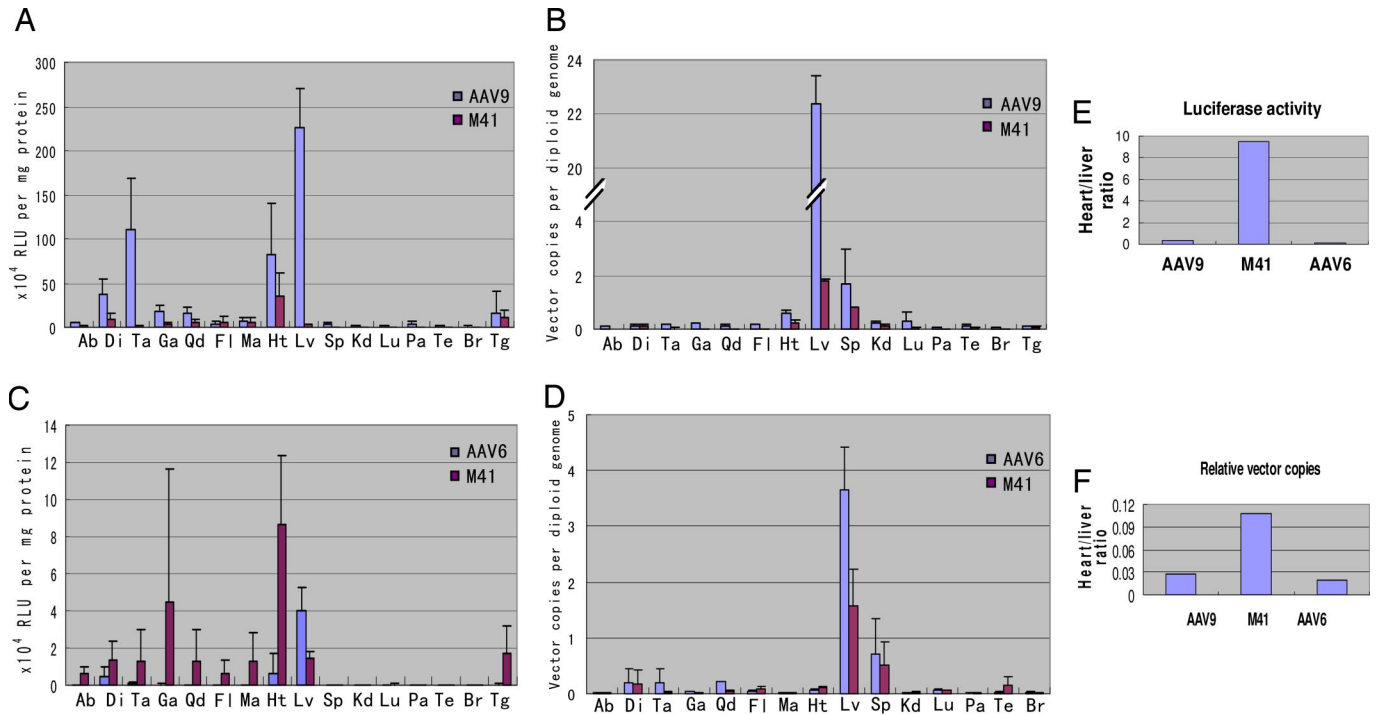


**Fig. 2.** Luciferase activities and vector genome copy numbers in various mouse tissues after systemic administration of AAV vectors. Comparison of AAV9- and AAVM41-CMV-Luc vectors in luciferase activities (A), and AAV vector genome copy numbers (B), at 2-weeks after i.v. injection of  $3 \times 10^{11}$  vector genomes in mice. Similar comparison of AAV6- or M41-CMV-Luc vectors in luciferase activities (C), and AAV genome copy numbers (D). Data are mean values  $\pm$  SD. Ab, abdomen muscle; Di, diaphragm; Ta, tibialis anterior; Ga, gastrocnemius; Qd, quadriceps; Fl, forelimb; Ma, masseter; Ht, heart; Lv, liver; Sp, spleen; Kd, kidney; Lu, lung; Pa, pancreas; Te, testis; Br, brain; Tg, tongue. Heart vs. liver ratio in transduction efficiency by 3 rAAV vectors on luciferase activities (E), and vector genome copy numbers (F).

X-gal staining in AAV9- and AAVM41-treated mice (Fig. 3). A similar test was also performed in hamsters, a different and larger species. At 3 weeks post i.v. injection into adult F1B hamsters, nearly 100% of the cardiomyocytes showed positive X-gal staining in both AAV9- and AAVM41-treated groups (Fig. 3). Quantitative enzyme assays showed nearly identical levels of LacZ expression in the hearts of AAV9- and AAVM41-treated mice as well as hamsters. In the skeletal muscles of the above mice and hamsters, however, AAVM41 was much less efficient than AAV9 (Fig. 3B). These results are consistent with those of luciferase reporter gene

transfer, suggesting preferential targeting of AAVM41 to the myocardium.

**Direct Infection of Cardiomyocytes and Skeletal Muscle by M41 Vector.** Since AAVM41 was initially isolated from the muscle but showed best infectivity to the heart after systemic delivery, we wished to examine the direct infectivity of AAVM41 on primary cardiomyocyte culture or on skeletal muscles by intramuscular injection. The AAV-LacZ vectors packaged by AAVM41, AAV6 and AAV9 were used to infect primary cardiomyocytes isolated

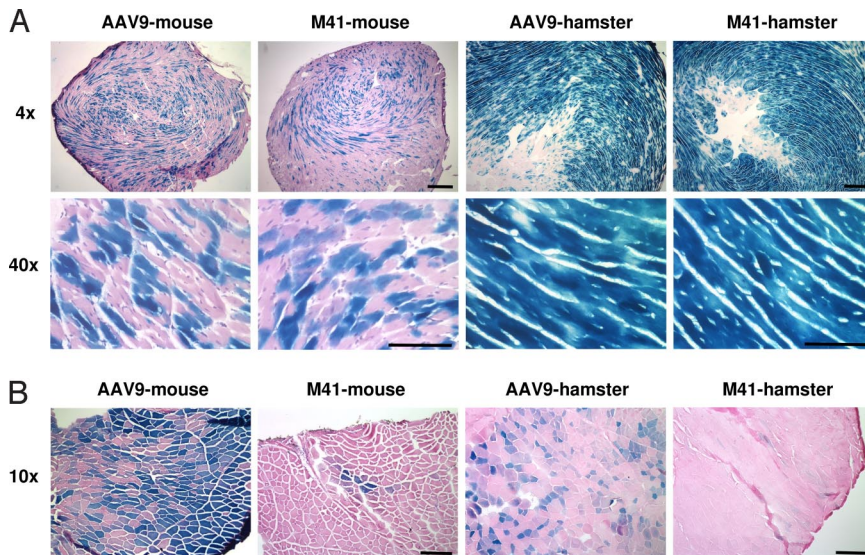


**Fig. 3.** Systemic delivery of LacZ transgene by AAVM41 into striated muscles. (A) X-gal staining of cross-sections of hearts after systemic administration of AAV vectors.  $3 \times 10^{11}$  vector genomes of AAV9- or M41-CB-LacZ were injected via tail vein into adult mice; and  $1 \times 10^{12}$  vector genomes of AAV9- or M41-CMV-LacZ were injected via jugular vein into adult hamsters. Hearts from mice or hamsters were collected at 2-weeks or 3-weeks post injection for X-gal and eosin staining. Two magnifications (4 $\times$  and 40 $\times$ ) were used for photography. (B) LacZ transgene expression in the tibialis anterior muscles of the same animals as described in (A). [Scale bars: A, 200  $\mu$ m (4 $\times$ ) and 50  $\mu$ m (40 $\times$ ); B, 100  $\mu$ m.]

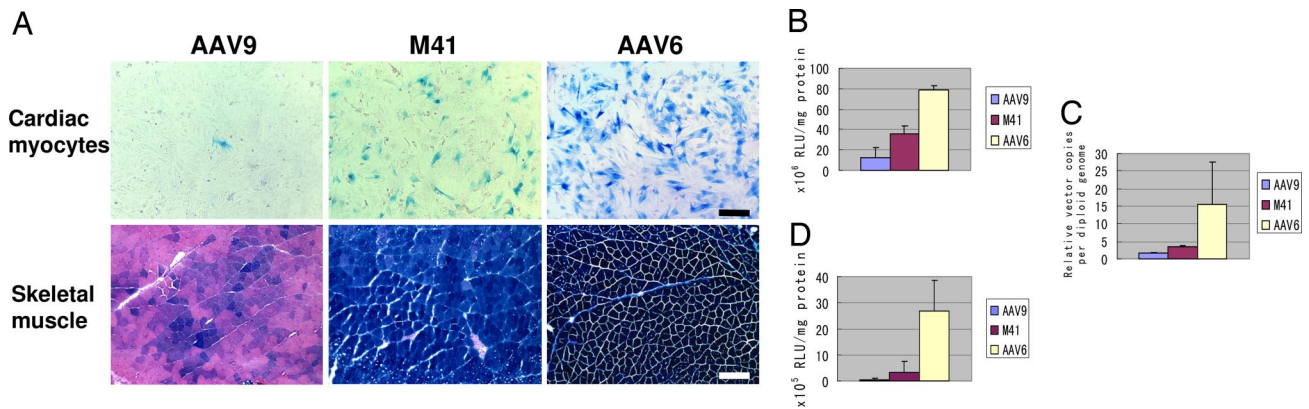


**Fig. 4.** Comparison of gene transfer efficiency in primary cardiomyocytes or skeletal muscles. (A) Representative X-gal staining of cardiomyocytes or skeletal muscle after transduction by AAV9-, AAVM41-, or AAV6-CMV-LacZ vectors. The AAV vectors were inoculated on the primary neonatal rat cardiomyocytes ( $5 \times 10^5$  cells per well) at an infection multiplicity of 3,000. Cells were fixed for X-gal staining 96 h later (Upper). The AAV vectors ( $5 \times 10^9$  v.g.) were also injected into the gastrocnemius muscle of adult C57BJ/6L mice and tissues were sectioned and stained with X-gal and eosin 14 days post-treatment (Lower). (Scale bars, 100  $\mu$ m.) (B and C) Quantitative  $\beta$ -gal activities and AAV vector genome copies in primary cardiomyocytes; and (D)  $\beta$ -gal activities in mouse skeletal muscles. Data are shown as mean values  $\pm$  SD.

from neonatal rats. Four days later, <1% of the AAV9-infected cardiomyocytes expressed the LacZ gene, but  $\approx$ 20% and 80% of the M41 and AAV6 cells, respectively, expressed the LacZ gene (Fig. 4A Upper). Quantitative analysis showed that  $\beta$ -gal enzyme activities of AAVM41- and AAV6-infected cardiomyocytes were 2.8-fold and 6.2-fold, respectively, of that of AAV9 (Fig. 4B). Similarly, the vector copy numbers in the cells were 2.3- and 10.3-fold of that of AAV9 (Fig. 4C). These data indicated that AAVM41 infectivity for cardiomyocytes was higher than AAV9 but lower than AAV6.

The above 3 AAV-LacZ vectors were then injected into mouse gastrocnemius muscle for comparison of skeletal muscle infectivities. Two weeks later, X-gal staining of the muscle cryosections revealed the strongest expression by AAV6, intermediate expression by AAVM41 and weak expression by AAV9 (Fig. 4A, lower panels). Quantitative  $\beta$ -gal activities of AAV6-injected muscles were 6.1-fold and 53.8-fold of that of AAVM41 and AAV9,

respectively (Fig. 4D). Together with the in vitro cardiomyocytes infection data, these results strongly suggest that the much improved systemic muscle and heart gene delivery by AAVM41 over AAV6 is most likely due to improved capability of crossing the tight endothelial barrier and reaching muscle cells.

**Application of M41 in a Cardiomyopathy and Congestive Heart Failure Hamster Model.**

Since AAVM41 showed preferential gene transfer in the heart, we next investigated the utility of this vector for gene therapy in a genetic cardiomyopathy and muscular dystrophy model, the  $\delta$ -sarcoglycan ( $\delta$ -SG) deficient TO-2 hamsters (9, 23). Four months after i.v. injection of  $1 \times 10^{12}$  v.g. of AAVM41- $\delta$ SG vector, SG expression was detected predominantly in the heart by immunofluorescent (IF) staining (Fig. 5A). Nearly 100% of the cardiomyocytes showed strong and uniform  $\delta$ -SG expression. However, only 10–30% of the skeletal muscle myofibers expressed  $\delta$ -SG, as shown in the forelimb, tibialis anterior and tongue muscles. Western

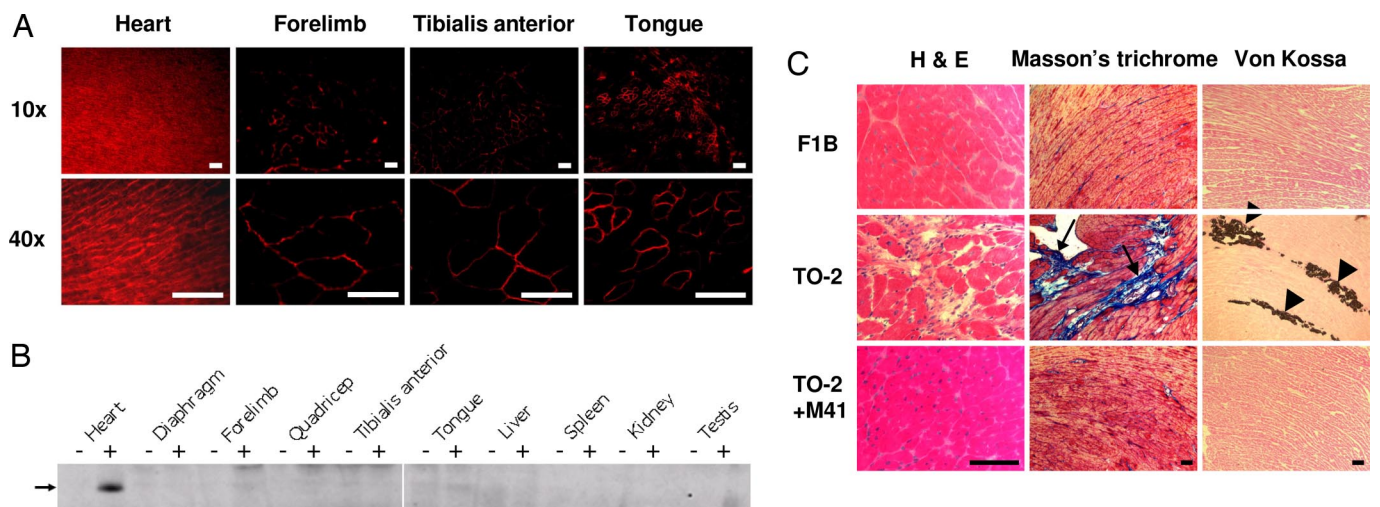


**Fig. 5.** Systemic delivery of  $\delta$ -sarcoglycan into cardiomyopathic hamster for treatment of heart failure. Totals of  $1 \times 10^{12}$  vector genomes of M41-Syn- $\delta$ SG vector were injected into 7-week-old male TO-2 hamsters via the jugular vein ( $n = 5$ ). (A) Immunofluorescent staining of  $\delta$ -sarcoglycan on thin sections of heart and skeletal muscle tissues 4 months after vector administration. Two magnifications were used for clear view. (Scale bars, 50  $\mu$ m.) (B) Western analysis of  $\delta$ -sarcoglycan in muscle and non-muscle tissues from untreated TO-2 (-) and rM41 vector-treated TO-2 (+) hamsters. Twenty micrograms of total proteins were loaded in each lane. (C) Amelioration of cardiomyopathy in TO-2 hamsters after  $\delta$ -sarcoglycan gene transfer. Hamster hearts of wild-type F1B, untreated TO-2 and AAVM41- $\delta$ SG-treated TO-2 were cryosectioned and stained with different methods for histology and pathology. Arrows and arrowheads indicate fibrosis and calcification, respectively. (Scale bars, 100  $\mu$ m.)

blot analysis confirmed strongest expression of  $\delta$ -SG in the heart (Fig. 5B). No  $\delta$ -SG expression was detected in the non-muscle tissues, including the liver. The muscle-specific, heart-preferential transgene expression was accompanied by the lack of immune rejection or toxicity throughout the duration of the experiments.

We also evaluated the therapeutic efficacies of AAVM41- $\delta$ -SG treatment in the TO-2 hamsters, which manifest both cardiomyopathy and muscular dystrophy. First, we measured serum levels of muscle creatine kinase activities and found no statistically significant difference between the treated and untreated groups, suggesting insufficient therapeutic gene transfer in the skeletal muscles by AAVM41. This is consistent with the IF staining results (Fig. 5A). We continued to examine the therapeutic efficacy on cardiomyopathy. Upon necropsy, gross examination of the untreated control TO-2 hamster hearts showed marked dilation and prominent calcification plaques. In contrast, the hearts of the treated TO-2 hamsters exhibited normal gross morphology, similar to those of wild-type control F1B hamsters. Histological staining further revealed large areas of cardiomyocyte degeneration (Fig. 5C, left panel), fibrosis (Fig. 5C, middle panel) or calcification (Fig. 5C, right panel) in the untreated TO-2 hamsters. However, those pathological signs were dramatically reduced or completely diminished in the AAVM41-treated hamster hearts. Echocardiography examination of the treated TO-2 hamsters also showed great improvement on all major parameters of cardiac functions, including left ventricle end-systolic dimension, percentage fractional shortening, and left ventricle posterior wall thickness, nearly identical to those of wild-type F1B hamsters, but significantly different from those of the untreated TO-2 hamsters ( $P < 0.05$  by Student's *t* test) (Fig. S1). These data further demonstrated the therapeutic efficacy by AAVM41 gene delivery in improving cardiac functions of TO-2 hamsters.

**Resistance of M41 to Pre-Existing Neutralizing Antibodies in Pooled Human IgGs.** Last, we investigated AAVM41 for its resistance to pre-existing neutralizing antibodies. Commercially available human IVIG (pooled human IgGs for i.v. use) was used as the source of antibodies (19, 20, 24, 25). AAVM41 was compared with AAV2, the best characterized serotype, and AAV8, a new isolate with low prevalence of pre-existing antibodies in human population (24, 25). The AAV2-, AAV8-, and AAVM41-LacZ vectors were pre-incubated with serial dilutions of IVIG, inoculated on Huh7 cell culture for 4 days and then assayed for LacZ expression as an indicator of vector resistance to neutralization (see *SI Materials and Methods* for details). At 1:64 dilution of IVIG, AAV2 infectivity decreased to  $33\% \pm 4\%$  of its control without IVIG. However, AAV8 and AAVM41 infectivities remained at  $94\% \pm 4\%$  and  $83\% \pm 1\%$  of their controls. Even at the highest IVIG concentration (1:8 dilution), AAV8 and AAVM41 still retained  $33\% \pm 12\%$  and  $26\% \pm 3\%$  of their infectivities, while AAV2 was nearly completely neutralized under the same condition (Fig. S2).

## Discussion

The purpose of this study was to retarget and optimize the tissue tropism of AAV vectors for striated muscles upon systemic delivery. Natural AAV1 and 6 are highly efficient in directly infecting striated muscles by local intramuscular (26, 27) or intramyocardial injection (28, 29), whereas AAV7, 8, and 9 are highly efficient in crossing the endothelial barriers in muscle and heart (5, 6, 30). To engineer vectors with combined properties, we generated AAV capsid gene libraries by DNA shuffling and performed direct *in vivo* selection. The major advantage of our study is the avoidance of bias and limitation of *in vitro* panning. We demanded simultaneous selection for viruses that are (i) efficient in crossing the endothelial barriers in the striated muscles; (ii) efficient in infecting muscle cells; and 3) poor in infecting the liver and other non-muscle cells. Direct *in vivo* screening and selection appeared to be the most desirable and feasible strategy. To this end, we have indeed

successfully generated a AAV capsid AAVM41, displaying mosaic capsid exterior surface with enhanced tropism to the striated muscles, especially the heart, and diminished infectivity to the liver.

The AAVM41 capsid achieved up to 13-fold improvement in the heart and several fold in the skeletal muscle by systemic gene transfer over its parental AAV6, which comprised a major portion of the C-terminal half of the capsid (Fig. 1). In addition, AAVM41 showed similar infectivity to the heart but a dramatic reduction to the liver, when compared to AAV9, the most efficient AAV vector for cardiac gene transfer by the systemic route. Despite the fact that AAVM41 showed diminished infectivity to the liver (Fig. 2), it is far from ideal. To further improve de-targeting AAVs from the liver, increasing selection stringency and specificity during *in vivo* panning, retrieving mutant AAVs from isolated cardiomyocytes or myofibers, instead of the whole tissue which contains a variety of non-muscle cells, could further enhance the screening efficiency. The use of extremely high-diversity libraries as the starting material by a combination of DNA shuffling and error-prone PCR could also increase the rate of success (19).

The precise mechanisms on how the liver and heart tropisms were altered for AAVM41 remain to be elucidated. We attempt to find explanations by analyzing its structural features contributed by the parental AAV serotypes (Fig. 1). The exterior surface of the AAVM41 viral particle was composed of loops from serotypes AAV1, 6, and 7 (Fig. 1B). The capsid surface should gain new properties on receptor/coreceptor binding and intracellular trafficking, thus, leading to the altered cell and tissue tropisms. The capsid C-terminal regions acquired from AAV1 and 6 may have played a crucial role in infectivity to the striated muscles, both skeletal and cardiac, whereas the N-terminal regions acquired from AAV7 and 8, mainly AAV7, may have improved systemic gene delivery with enhanced transcytosis across the endothelial cell lining (5, 31). While the AAV6 might stay in endothelial cells after intravascular delivery, AAVM41 could transcytose into the extravascular space and efficiently infect muscle cells. Characterization of AAVM41 interaction with endothelial and muscle cells and potential cellular receptors should shed light on its evolution and future improvement. Finally, the myocardium specificity can be strengthened by the use of cardiac-specific promoters, and resistance of AAVM41 to pre-existing antibodies could be further enhanced by additional selections (19, 20).

## Materials and Methods

**Generation of Chimeric AAV Library with Shuffled Capsid Genes.** For construction of random chimeric AAV capsid gene libraries, AAV serotypes 1, 2, 3B, 4, 6, 7, 8, and 9 were used as PCR templates. The capsid genes were amplified by primers CAP-5' (5'-CCC-AAGCTTCGATCAACTACGACAGGATACCAA-3') and CAP-3' (5'-ATAAGAAT-GCGGCCG-AGAGACCAAAGTCAACTGAAACGA-3') and mixed in equal ratio for DNA shuffling (18). In brief, 4  $\mu$ g of the DNA templates were treated by 0.04 U of DNase I at 15 °C briefly. DNA fragments in size of 300–1,000 bp were purified by agarose gel electrophoresis, denatured, reannealed and repaired by *pfu* DNA polymerase to reassemble random capsid genes. Amplification was done by use of *pfu* DNA polymerase and CAP5'/CAP3' primers. The PCR program was 30 cycles of 94 °C 1 min, 60 °C 1 min and 72 °C 4.5 min. The PCR products were then digested with HindIII and NotI and ligated into a HindIII and NotI digested plasmid backbone containing AAV2 *Rep* gene and inverted terminal repeats. The random infectious plasmids library was obtained by transforming the above ligated DNA into DH10B *E. coli* cells. Random clones were picked for restriction enzyme analysis and replication and packaging viability in 293 cells. The shuffled infectious AAV library was finally produced using a self-packaging technique developed by Muller *et al.* (22).

**In Vivo Bio-Panning of Mutant AAV Capsid Library in Mice.** A dose of  $5 \times 10^{11}$  vector genomes of the chimeric AAV library were injected into adult C57BL/6J mice via tail vein. Three days later, mice were killed and perfused with PBS to remove the blood from tissues. The hind limb skeletal muscles and liver were collected for total DNA isolation. The capsid genes enriched in the muscle were retrieved by PCR amplification using primers Cap 5' and Cap 3' and the iProof DNA polymerase (Bio-Rad). The PCR products were digested with HindIII and NotI and cloned similarly as described in previous section. The 43 representative AAV

capsid genotypes were identified from the reconstructed plasmid library by restriction analysis and mixed in equal ratio for production of a secondary AAV library as described earlier. This AAV library was again injected i.v. in mice for secondary screening and retrieval from muscle and liver. Random colonies were sequenced and compared for their tissue distribution.

**Sequence and Structure Analyses of Modified AAV Capsid Genes.** Identification and alignment of the capsid genes from the mouse tissues was done using Clustal X (32). A 3D homology model of the VP3 structure of AAVM41 was generated from the coordinates of the crystal structures of AAV1, AAV7, and AAV8 (17) and a homology model of AAV6 (33), the parental viruses, using the Coot program (34). After superimposition of these template coordinates, the chimeric M41 VP3 structural model was generated by manual cutting and pasting of the appropriate amino acid sequences from each serotype and regularization of the model geometry. To visualize the contribution of each serotype in the context of the assembled M41 capsid icosahedral 2-, 3-, and 5-fold symmetry operators were applied to the VP3 model coordinates by matrix multiplication using the program O (36). The serotype segments were then highlighted in the context of 9 VP3 monomers which surround 1 viral asymmetric unit in a surface rendered depiction generated using the program PyMol (35).

**Tissue Tropism of AAV Vectors in Mice after Systemic Administration.** The M41 capsid gene was used to package CMV-luciferase, CB-LacZ, or CMV-LacZ reporter vectors for comparison with the AAV9 or AAV6 packaged ones. Three  $\times 10^{11}$  v.g. of reporter vectors containing CMV-luciferase or CB-LacZ genes were injected i.v. into 6- to 8-week-old C57BL/6J mice for systemic gene delivery and expression. The heart, skeletal muscle and main internal organs of mice were collected 2 weeks later. Reporter gene expression was monitored by luciferase assay (Luciferase Assay System; Promega) or  $\beta$ -gal assay (Galacto-Light Plus™ system; Applied Biosystems). Cryosectioning and X-gal staining were used to visualize cells that expressed the LacZ in the heart and muscle. Total DNA was extracted from mouse

tissues for quantitative detection of vector genome copies by Taqman probes (Applied Biosystems) with a single-copy endogenous gene (glucagon gene) as the diploid cell number reference.

**Transduction of Primary Cardiomyocytes or Skeletal Muscle by AAV Vectors.** Rat neonatal cardiomyocytes were isolated and cultured as previously reported (37). Twenty-four hours after preplating, rAAV9-, rM41-, or rAAV6-CMV-lacZ vectors were inoculated onto the cardiomyocytes in infection multiplicity of 3000. Cells were fixed for X-gal staining or  $\beta$ -gal assay after another 96 h to detect transgene expression. For skeletal muscle transduction, 50  $\mu$ L of virus dilutes containing  $5 \times 10^9$  v.g. of rAAV vectors were intramuscularly injected into gastrocnemius muscles of adult 7-week-old C57BL/6L mice. Fourteen days later muscle tissues were collected for detection of transgene expression by X-gal staining or  $\beta$ -gal assay. Vector genome distribution in cardiomyocytes or skeletal muscles was quantitated by real-time PCR as described.

**Gene Transfer and Functional Assays in the Hamster Models.** Tropism of the vectors in hamsters was first investigated in the normal F1B hamsters. A dose of  $10^{12}$  vector genomes of M41-CMV-lacZ or AAV9-CMV-lacZ was administered into 2- to 3-month-old male F1B hamsters via the jugular vein. Three weeks later, heart, skeletal muscles, and the internal organs, including the liver, were collected for histological staining. The synthetic muscle-specific promoter (SYN) C5-12 was used to achieve strong and muscle-specific  $\delta$ -5G transgene expression in the TO-2 hamsters (9). A dose of  $10^{12}$  vector genomes of the M41-SYN- $\delta$ 5G vectors were administered into 7-week-old male TO-2 hamsters intravenously with untreated TO-2 or with normal F1B hamsters as the control groups. Characterizations of Sarcoglycan expression, histology examination, and function test were done according to the previous publication (9).

**ACKNOWLEDGMENTS.** We thank Dr. Tong Zhu for his technical support in vector administration. This work was supported by National Institutes of Health grants AR45967 and AR50595 to X.X., AI72176 to MAM., and HL85635 to DW.

- Goodwin FC, Muntoni F (2005) Cardiac involvement in muscular dystrophies: Molecular mechanisms. *Muscle Nerve* 32:577–588.
- McNally EM (2007) New approaches in the therapy of cardiomyopathy in muscular dystrophy. *Annu Rev Med* 58:75–88.
- Xiao X, Li J, Samulski RJ (1996) Efficient long-term gene transfer into muscle tissue of immunocompetent mice by adeno-associated virus vector. *J Virol* 70:8098–8108.
- Li J, et al. (2003) Efficient and long-term intracardiac gene transfer in delta-sarcoglycan-deficiency hamster by adeno-associated virus-2 vectors. *Gene Ther* 10:1807–1813.
- Wang Z, et al. (2005) Adeno-associated virus serotype 8 efficiently delivers genes to muscle and heart. *Nat Biotech* 23:321–328.
- Pacac CA, et al. (2006) Recombinant adeno-associated virus serotype 9 leads to preferential cardiac transduction in vivo. *Circ Res* 99:e3–9.
- Jiang H, et al. (2006) Evidence of multiyear factor ix expression by aav-mediated gene transfer to skeletal muscle in an individual with severe hemophilia b. *Mol Ther* 14:452–455.
- Mueller C, Flotte TR (2008) Clinical gene therapy using recombinant adeno-associated virus vectors. *Gene Ther* 15:858–863.
- Zhu T, et al. (2005) Sustained whole-body functional rescue in congestive heart failure and muscular dystrophy hamsters by systemic gene transfer. *Circulation* 112:2650–2659.
- Gregorevic P, et al. (2006) rAAV6-microdystrophin preserves muscle function and extends lifespan in severely dystrophic mice. *Nat Med* 12:787–789.
- Gao G, et al. (2003) Adeno-associated viruses undergo substantial evolution in primates during natural infections. *Proc Natl Acad Sci USA* 100:6081–6086.
- Gao G, et al. (2004) Clades of adeno-associated viruses are widely disseminated in human tissues. *J Virol* 78:6381–6388.
- Inagaki K, et al. (2006) Robust systemic transduction with aav9 vectors in mice: Efficient global cardiac gene transfer superior to that of aav8. *Mol Ther* 14:45–53.
- Gao G, et al. (2002) Novel adeno-associated viruses from rhesus monkeys as vectors for human gene therapy. *Proc Natl Acad Sci USA* 99:11854–11859.
- Xie Q, et al. (2002) The atomic structure of adeno-associated virus (aav-2), a vector for human gene therapy. *Proc Natl Acad Sci USA* 99:10405–10410.
- Govindasamy L, et al. (2006) Structurally mapping the diverse phenotype of adeno-associated virus serotype 4. *J Virol* 80:11556–11570.
- Nam HJ, et al. (2007) Structure of adeno-associated virus serotype 8, a gene therapy vector. *J Virol* 81:12260–12271.
- Soong NW, et al. (2000) Molecular breeding of viruses. *Nat Genet* 25:436–439.
- Maheshri N, Koerber JT, Kaspar BK, Schaffer DV (2006) Directed evolution of adeno-associated virus yields enhanced gene delivery vectors. *Nat Biotech* 24:198–204.
- Grimm D, et al. (2008) In vitro and in vivo gene therapy vector evolution via multispecies interbreeding and retargeting of adeno-associated viruses. *J Virol* 82:5887–5911.
- Li W, et al. (2008) Engineering and selection of shuffled aav genomes: A new strategy for producing targeted biological nanoparticles. *Mol Ther* 16:1252–1260.
- Muller OJ, et al. (2003) Random peptide libraries displayed on adeno-associated virus to select for targeted gene therapy vectors. *Nat Biotech* 21:1040–1046.
- Nigro V, et al. (1997) Identification of the syrian hamster cardiomyopathy gene. *Hum Mol Genet* 6:601–607.
- Scallan CD, et al. (2006) Human immunoglobulin inhibits liver transduction by aav vectors at low aav2 neutralizing titers in scid mice. *Blood* 107:1810–1817.
- Lin J, Calcedo R, Vandenberghe LH, Figueredo JM, Wilson JM (2008) Impact of preexisting vector immunity on the efficacy of adeno-associated virus-based hiv-1 gag vaccines. *Hum Gene Ther* 19:663–669.
- Chao H, et al. (2000) Several log increase in therapeutic transgene delivery by distinct adeno-associated viral serotype vectors. *Mol Ther* 2:619–623.
- Blankinship MJ, et al. (2004) Efficient transduction of skeletal muscle using vectors based on adeno-associated virus serotype 6. *Mol Ther* 10:671–678.
- Su H, et al. (2008) AAV serotype 1 mediates more efficient gene transfer to pig myocardium than AAV serotype 2 and plasmid. *J Gene Med* 10:33–41.
- Palomeque J, et al. (2007) Efficiency of eight different aav serotypes in transducing rat myocardium in vivo. *Gene Ther* 14:989–997.
- Zincarelli C, Soltys S, Rengo G, Rabinowitz JE (2008) Analysis of AAV serotypes 1–9 mediated gene expression and tropism in mice after systemic injection. *Mol Ther* 16:1073–1080.
- Di Pasquale G, Chiorini JA (2005) AAV transcytosis through barrier epithelia and endothelium. *Mol Ther* 13:506–516.
- Larkin MA, et al. (2007) Clustal w and clustal x version 2.0. *Bioinformatics* 23:2947–2948.
- Padron E, et al. (2005) Structure of adeno-associated virus type 4. *J Virol* 79:5047–5058.
- Emsley P, Cowtan K (2004) Coot: Model-building tools for molecular graphics. *Acta Crystallogr D Biol Crystallogr* 60:2126–2132.
- DeLano WL (2002) Unraveling hot spots in binding interfaces: Progress and challenges. *Curr Opin Struct Biol* 12:14–20.
- Jones T, et al. (1991) Improved methods for building protein models in electron density maps and the location of errors in these methods. *Acta Crystallogr A* 47:110–119.
- Callis TE, et al. (2005) Bone morphogenetic protein signaling modulates myocardial transactivation of cardiac genes. *Circ Res* 97(10):992–1000.